# Optimal Design and Verification of a PM Synchronous Generator For Wind Turbines

Yucel Cetinceviz*‡, Durmus Uygun**, Huseyin Demirel***

* Mechatronics Dept., Kastamonu University, Kastamonu, Turkey

** Aegean Dynamics Corp., Dokuz Eylul University Technopark, Izmir, Turkey

*** Electrical-Electronics Eng. Dept., Karabuk University, Karabuk, Turkey

(ycetinceviz@kastamonu.edu.tr, durmus.uygun@aegeandynamics.com, hdemirel@karabuk.edu.tr)

‡ Corresponding Author; Yucel Cetinceviz, Kastamonu, Turkey, Tel: +90 366 215 0900,
Fax: +90 366 215 0898, ycetinceviz@kastamonu.edu.tr

*Received: 21.02.2017 Accepted:04.06.2017*

**Abstract-** This study reports the analytical computation including performance characteristics under no-load condition in combination with coupled 2D electromagnetic field-circuit analysis of a 4kW direct drive permanent magnet synchronous generator (PMSG) to be used in micro-scale wind turbine applications. The specifications such like stack length, skew and magnet offset of PMSG are optimized by using parametric approach including multi-objective design optimization. It describes the methodology to gain required output performance such as output power, load voltage and maximum efficiency of the wind generator. Based on the optimized design, the model has been exposed to some transient coupled-field circuit analyses based on variable wind flow speed under no-load conditions. In addition to these evaluations; the experimental results verified the effectiveness of the employed simulations model related to finite element methods and analytical studies showing that that the induced voltage at nominal speed and no-load condition is at desired level and results obtained under no-load condition are in good agreement with the analysis and analytical results.

**Keywords** wind turbine, coupled-circuit analysis, PM generator, multi-objective design optimization, parametric approach, reluctance model.

## 1. Introduction

The need for the energy is increasing day by day along with rapid population growth and industrialization. The fossil fuels such as coal, oil and natural gas which are used to meet these requirements are being replaced by renewable energy sources like sun, wind, geothermal, hydraulic and ocean resources [1-7].

In such kinds of power plants; commonly variable speed permanent magnet synchronous generators (PMSGs) [8-16] and doubly-fed induction generators (DFIGs) [7, 17] are employed. Variable-speed turbine structure housing PM generator offers appropriate solutions to meet the energy needs of the rural areas. Many studies have been carried out on the design of PM generator for wind turbine application [18-24]. In one of these, a designed 4-kW air-cored radial flux PM wind generator has been used in a direct battery-charging system [18]. In another study, large direct-drive wind turbines with cost effective PM generator systems have been designed with combinations of rated power ranges from 100 kW to 10 MW [22]. The optimum results have been presented and compared according to the performance of the annual energy output per cost [22].

Mostly, the grid-connected large scale wind generators are marketed and installed today in the world [22, 23]. Simultaneously, there is a need for smaller wind power applications for usage in hybrid energy systems to meet the energy needs of eco-house and eco-business concepts, such as houses, petroleum offices, farms and small businesses [23]. Large scale wind turbine generators consist of a low speed range 15 to 100 rpm, while small-scale wind turbines include low speeds range 150 to 500 rpm in wind power plant. PMSGs are one of the best solutions for small scale wind power plants [23].

The objective of this article is related to present the electromagnetic design and transient performance analysis of a 4kW PMSG to get maximum available energy from wind. To gain maximum available energy, detailed design and analysis was carried out to cover the operational aspects such as start-up torque, cogging torque, ripple, efficiency, rated power and terminal voltage. The electromagnetic design methodology of PM synchronous

machines has been studied in the literature. The air gap magnetic field density provides important characteristics for machine design and performance prediction [25, 26]. A general approach is to use finite element model (FEM). But it is a time-consuming solution. The other approach is to use a magnetic vector potential formulation which is used in 2D polar coordinates to describe the flux density distribution in the machine [8, 25, 26]. Another approach is the usage of magnetic circuit model including reluctance or permanence model of the machine [22, 23 and 27-31]. In this paper, a radial flux surface mounted permanent magnet synchronous generator has been modelled analytically based on magnetic circuit (reluctance model) for machine design and performance prediction. The cogging torque is a common issue for permanent magnet machines [14]. The torque ripple in the cogging torque is related to the harmonics in the back-EMF. To reduce it, the effect of the slot opening, the magnet thickness and the pole arc/magnet arc ratio (embrace) of the cogging the torque were investigated parametrically in [32].

In this study, the effect of stack length, skew and magnet offset on the cogging torque, efficiency, output power and terminal voltage were investigated parametrically as well. Thus, this study gives an opportunity to analyze transient performance of 4 kW PMSG under no-load and variable generator speed rates related to wind speed by using coupled two dimensional (2D) electromagnetic field-circuit model. In addition to this, the experimental studies were carried out to verify the simulations model and analytical results. One of the most significant contribution of the paper is that the analytical model is also evaluating linear topology of the generator along with magnetic circuit model which is considering some estimations and simplifications of the machine geometry and combining it with two-dimensional coupled electromagnetic field-circuit approach.

## 2. Design Process

### *2.1. Machine Topology and Sizing Equations*

Based on the placement of the magnets on the rotor, generally a typical permanent magnet synchronous machine can be classified into three types, such as interior PM synchronous machines which have the permanent magnets buried inside the rotor, surface PM synchronous machines which are required to shape the magnets into the form, placed on the rotor outer surface[33], and inset PM synchronous machines in which the permanent magnets are inset into the rotor. And also based on the flux directions for the airgap, the structure can also be divided into two configurations type, so called radial or axial for surface type configuration where magnetic flux crosses the airgap in radial direction and it crosses the air gap in axial direction in the other type [8, 34, 35].

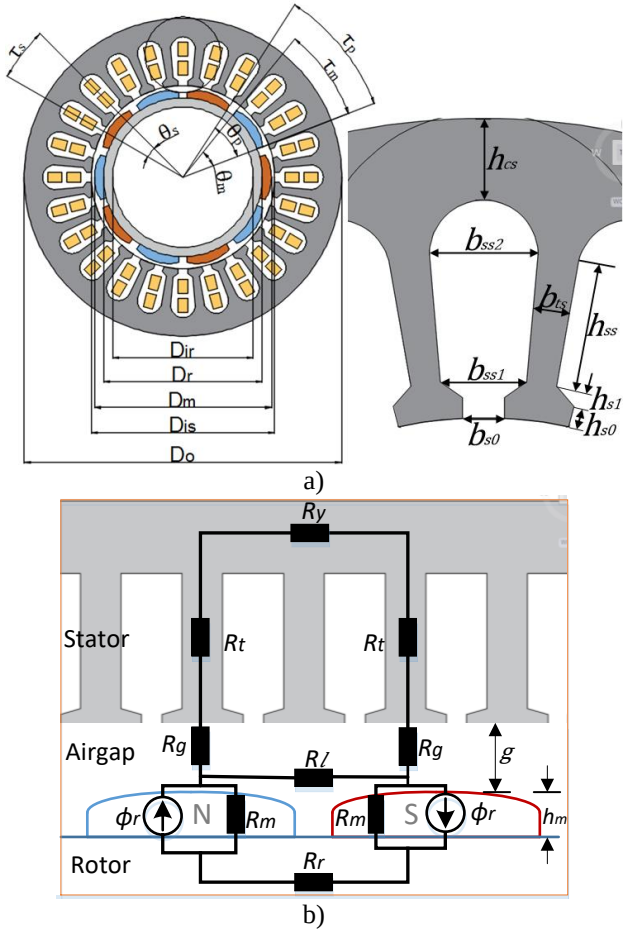


**Fig.1.** Topology of radial flux wind generator: a) PMSG topology; b) Linear topology and magnetic circuit model for the structure

In this construction; the air gap is perpendicular to the rotational axis. The most conventional PM machines are constituted by placing the PM's on the rotor surface because of the simplest construction. In this paper; PMSG is designed based on the surface mounted rotor construction [27] as shown Fig.1.

An electric machine design starts by explaining the relationship between the main dimensions of the machine and performance of the machine. It is necessary to specify a few initial parameter such as output power, nominal speed, number of poles of the machine, material data of the stator, rotor, magnet type and conductors for the design. These specifications are given in Table 1.

**Table 1.** Given Initial Data for the PMSG

| Technical Data of PMSG for Wind Turbine | |
|---|---|
| Rated output power (kW) | 4 |
| Rated speed (rpm) | 250 |
| Frequency (Hz) | 50 |
| Number of poles | 24 |
| Number of phases | 3 |
| Rated voltage (V) | 400 |
| Rated power factor | 0.95 |
| Target efficiency | >= %92 |
| Shaft material | ASTM316 |

| | Stainless steel |
|---|---|
| Rotor frame | SD52 |
| Stator frame | Aluminum (cast iron) |
| Stator lamination | M19 (M310-50A) |
| Magnet (NdFeB)<br>Remanent flux density $B_r$ (T)<br>Relative Recoil Permeability $\mu_{rec}$ Coercivity $H_c$ (kA/m)<br>Temperature (max °C) | N40SH (nickel-plating)<br>1.28<br>1.05<br>989<br>150 |

According to basic dimensioning process, at first it is necessary to determine the main dimensions of the machine; the stator bore diameter or air-gap diameter ($D_{is}$) and the equivalent core length ($L$). For this, it is necessary to explain the relation between $D_{is}^2 L_{stk}$ and the output power of the machine [36]. The analytical calculations required to determine these parameters were performed in the literature [27, 32 and 36-40] . However; specific magnetic ($A$) and electric loading ($B_g$) can initially be estimated as follows for the sizing procedure of electrical machines [30];

- $B_g$ = (0.7T …. 0.9T) $B_r$ [38] or 0.8T to 1T [40] for medium power machines.
- $A$ ranges from 10 to 55 kA/m [38] or 10 to 40 kA/m [37, 39] for medium power machines.

For stator sizing, slot depth $h_{ss}$, stator core heights $h_{cs}$ and widths of the stator tooth $b_{ts}$ can be estimated respectively as follows [21, 27, 36, 37, 39];

$$h_{ss} = \frac{A}{\frac{B_g}{B_{sat}} j_{con} K_{fill}} \tag{1}$$

$$h_{cs} = \frac{\alpha_i}{2}\left(\frac{\pi D_{is}}{2p}\right)\frac{B_g}{B_{sat}} \tag{2}$$

$$b_{ts} = \frac{\tau_s}{K_{sf}} \cdot \frac{B_g}{B_{sat}} \tag{3}$$

$$\tau_s = \frac{\pi D_{is}}{Q_s} \tag{4}$$

Where, $B_{sat}$ is the iron saturation flux density and $B_g$ is the airgap flux density, $J_{con}$ is current density, $K_{fill}$ is the slot fill factor, $K_{sf}$ is the stacking factor of the stator laminations and $p$ is the number of pole pairs. The shape factor $\alpha_i$ is defined as the ratio of the average-to-maximum value of the air gap flux density. The slot pitch $\tau_s$ is given by equation (4) where $Q_s$ is the slot number. As shown in Fig. 1; the lower and upper side of slot width can be calculated respectively as follows [36, 41];

$$b_{ss1} = \pi \frac{(D_{is} + 2\times h_{s0} + 2\times h_{s1})}{Q_s} - b_{ts} \tag{5}$$

$$b_{ss2} = \pi \frac{(D_{is} + 2\times h_{s0} + 2\times h_{s1} + 2\times h_{ss})}{Q_s} - b_{ts} \tag{6}$$

For rotor and PM material sizing; the height of the rotor core $h_{cr}$ and the height of the NdFeB PM material $h_m$ per pole required for a synchronous machine design can be expressed respectively as [27, 37, 39, 42];

$$h_{cr} = \frac{\alpha_i}{2}\left(\frac{\pi(D_{is} - 2h_m)}{2p}\right)\frac{B_g}{B_{sat\_r}} \tag{7}$$

$$h_m = \mu_{rrec} \cdot \frac{B_g / K_{lm}}{B_r - B_g / K_{lm}} \cdot g \tag{8}$$

Where $g$ is the rectangular air gap length, $K_{lm}$ is a *coefficient of leakage flux* that is typically in the range 0.9 to 1.0 for the surface magnets [43], $B_r$ is the remanent flux density, $\mu_{rec}$ is the relative recoil permeability of magnets. For the initial design, the height of the magnet can be determined to be about ten times the air gap length [44].

### *2.2. Analytical Model of PMSG*

Electric machines are usually analytically modeled on the basis of some estimations and simplifications of the machine geometry and material properties of machine [28]. Machine design studies mostly involve finite element methods (FEM) simulations. By the reason that a FEM gives more accurate results than analytical model, but it is a disadvantage that the calculation time is long. [35].

No-load air gap flux density is one of the most important characteristics for machine design and performance prediction [45]. Therefore, the magnetic circuit model is used to obtain the air gap flux density as shown Fig.1b. First of all, it is necessary to define the main flux paths and determine the reluctances of the magnetic circuit. So, the magnetic circuit of the generator is divided into five parts which are stator yoke reluctance $R_y$, stator teeth reluctance $R_t$, air gap reluctances $R_g$, magnet reluctances $R_m$ and leakage between the magnets $R_l$ and rotor yoke reluctances $R_r$. Reluctances are located in a pole pitch as shown in Fig.1b.

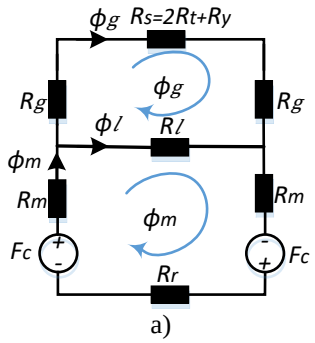

a)

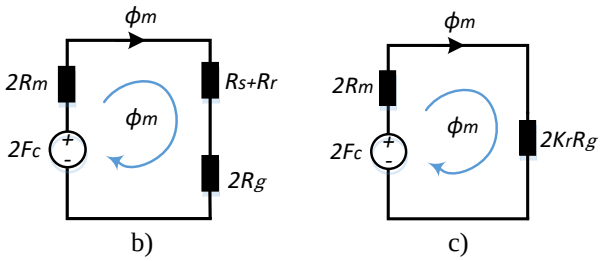


**Fig.2.** Simplifications of the magnetic circuit

Fig.2 shows the equivalent magnetic circuit [31] called as Reluctance Model (RM) and its simplified model. In this illustration, the stator and rotor steels are modeled as reluctances $R_s$ and $R_r$, respectively. $R_s$ contains stator yoke reluctance and stator teeth reluctance and three circuit fluxes which the magnet flux $\phi_m$, air gap flux $\phi_g$, and leakage flux $\phi_l$. For this model the magneto motive force $F_c$ and remanent flux $\phi_r$ of the permanent magnets according to demagnetization curve can be calculated as follow;

$$F_c = h_m H_c \tag{9}$$

$$\Phi_r = B_r A_m \tag{10}$$

The flux depends on the material properties as well as on the magnet dimensions. Where $A_m$ is the magnet pole area and $H_c$ is the coercivity of the magnets.

To calculate the back emf, the air gap flux density $B_g$ must be determined firstly. The air gap flux can be obtained in terms of the magnet flux as $\phi_g = K_{lm}.\phi_m$. Where $K_{lm}$ is a *coefficient of leakage flux* that is typically in the range 0.9 to 1.0 for the surface magnets [43]. In the other references [30, 44]; it is defined as the ratio of airgap flux to magnet flux:

$$K_{lm} = \frac{\Phi_g}{\Phi_m} = \frac{\Phi_g}{\Phi_g + \Phi_l} < 1 \tag{11}$$

In another study [38]; this parameter has been defined as the ratio of magnet flux to airgap flux ($K_{lm}>1$) and $\phi_g = \phi_m / K_{lm}$. Then by eliminating the leakage reluctance $R_l$ and the steel reluctances ($R_s$ and $R_r$) by introducing a *reluctance factor* $K_r$, the magnetic circuit can be simplified as shown Fig.2c. The magnetic flux can be obtained using electric circuit principles which is called Kirchhoff's voltage law (KVL) to the loops in Fig.2c as follows [46, 47]:

$$\Phi_m = \frac{2F_c}{2R_m + 2K_r R_g} = \frac{2R_m}{2R_m + 2K_r R_g}\Phi_r \tag{12}$$

Based on $\phi_g = \phi_m / K_{lm}$, the flux density relationships $B_g = \phi_g / A_g$ and $B_r = \phi_r / A_m$, the air gap flux density can be obtained as [29, 30, 43, 44];

$$B_g = \frac{K_l}{1 + K_r \dfrac{R_g}{R_m}} \frac{A_m}{A_g} B_r \tag{13}$$

The magnet and air gap reluctances are given respectively by [29, 30, 43, 44];

$$R_m = \frac{h_m}{\mu_{rec}\mu_0 A_m} = \frac{h_m}{\mu_{rec}\mu_0 \tau_m L_{stk}} \tag{14}$$

$$R_g = \frac{g}{\mu_0 A_g} = \frac{g}{\mu_0 \tau_p L_{stk}} \tag{15}$$

Where $A_m$ is the magnet area, $A_g$ is the gap area of one pole pitch, $\tau_m$ is the magnet pitch and $\tau_p$ is the pole pitch [35]. Thus substituting the reluctance expressions in (14) and (15) to (13); the air gap flux density can be written as [29, 30, 43, 44];

$$B_g = \frac{K_l C_\phi}{1 + K_r \dfrac{\mu_{rec}}{P_c}} B_r \tag{16}$$

No-load induced phase voltage called as back-EMF can be calculated by multiplying the air gap flux density and the winding turns in stator per phase as follows [22, 28, 30, 35, 44].

$$E_p = \frac{\omega_m k_w N_s \Phi_g}{\sqrt{2}} = \frac{\omega_m k_w N_s \alpha_i B_g \pi D_r L_{stk} / 2p}{\sqrt{2}} \tag{17}$$

Where $\omega_m$ is the mechanical angular speed of the rotor, $k_w$ is the winding factor, $p$ is the number of pole pairs, $D_r$ is the rotor diameter, $N_s$ is the number of turns of the phase winding and the saturation form factor is $\alpha_i = 2/\pi$.

In direct-drive generators concept, designed generators can be used in very low speed applications. So, the effect of cogging torque is very important. The cogging torque can be obtained using the magnetic energy stored in the air gap and PMs of machine as follows [48-50]:

$$\begin{aligned} T_{cog}(\theta) &= -\frac{\partial W}{\partial \theta} \\ &= -\frac{\pi Q L_{stk}}{4\mu_0}(R_2^2 - R_1^2)\sum_{n=1}^{\infty} n G_{sn} B_{sn} \sin nQ\theta \end{aligned} \tag{18}$$

Where $R_2$ and $R_1$ are the inner radius of armature and the outer radius of rotor, respectively; $Q$ is the number of slots and $\theta$ is the rotor position. The expressions of Fourier expansion coefficients $G_{sn}$ and $B_{sn}$ are detailed in [48, 49].

### *2.3. Multi-Objective Optimization*

In this paper, the addressed optimization problem for the fundamental electromagnetic design can be expressed by a simple function as [20, 32, 51]:

$$y = f(x_i), i = 1, 2, 3..... \tag{19}$$

Where $y$ is one of the output performance parameters of generator; $x_i$ is the sizing or structural parameters of the related generator dimension in iteration. To achieve optimum generator design, output power, efficiency, load line voltage, cogging torque and etc. of the generator is

selected as the multi-objective optimization. The structural parameters are selected as input-free parameters which obtained by calculations, such as slot opening value $b_{so}$, pole pitch/magnet pitch ratio $\tau$, the height of magnet $h_m$ in [32], and also the stack length $L_{stk}$, skew and offset magnet in this paper. The multi-objective optimization approach of which main idea can be obtained in [20, 32]:

$$\begin{Bmatrix} \text{maximize} \rightarrow y = f(h_m, \alpha_m, b_{so}, L_{stk}, skew, offset) \\ \text{or} \\ \text{minimize} \rightarrow P_{loss} = f(h_m, \alpha_m, b_{so}, L_{stk}, skew, offset) \\ \text{related to} \rightarrow \begin{Bmatrix} 70mm \le L_{stk} \le 115mm, ++5mm \\ 0 \le skew \le 1, ++0.2 \\ 70mm \le offset \le 90mm, ++2mm \end{Bmatrix} \end{Bmatrix} \quad (20)$$

The analysis shown in Fig.3 includes the study on the sizing of stator core and the improvement of initial parameters. At rated speed (250 rpm) and for 115 mm stack length, the generator efficiency is about 92%, but when the stack length is reduced to 70mm, the efficiency increases to 93.5% for lower power ratio. When lower stack length increases the efficiency, it causes the line voltage to be less than 400V.

In direct drive generators, the effect of cogging torque is considerably significant since the designed generators may be used in very low speed application. One of the methods to eliminate cogging torque is "skewing of either stator slots or magnets" in which we preferred magnet skewing owing to easy manufacturing cases [32]. Fig.4 shows the effect of variable *skew* on load line voltage, output power, efficiency and cogging torque parameter of generator. The value of the skew is taken as 1 to minimize the cogging torque and the fact remains that it still provides desired machine performance.

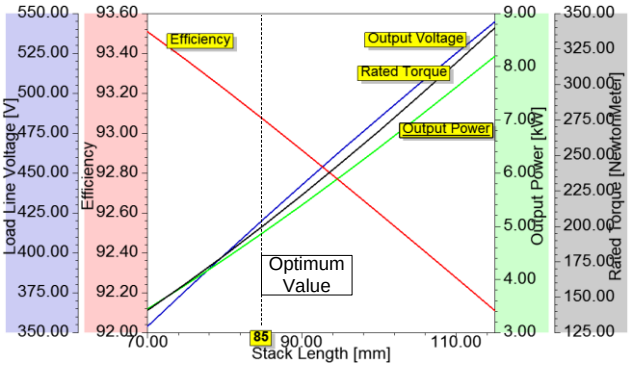


**Fig. 3.** Effect of variable stack length $L_{stk}$ on load line voltage, output power, efficiency and rated torque parameter of generator.

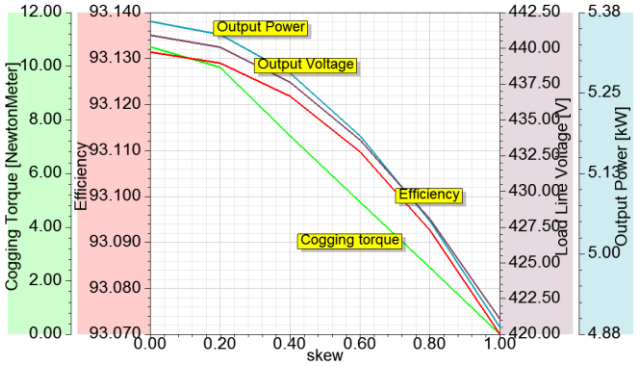


**Fig. 4.** Effect of variable *skew* on load line voltage, output power, efficiency and cogging torque parameter of generator.

The quality back EMF can be further increased by using the arc shaped magnet as shown Fig.5. The effect of variable *offset* and *skew* on THD of back emf as shown Fig.6. It clearly shows that the value of the THD of back emf decreases as the *offset* and *skew* values increase.

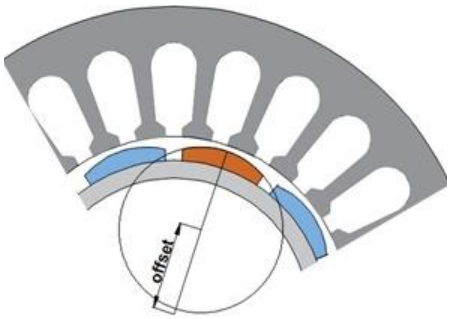


**Fig. 5.** The optimization according to magnet offset [18].

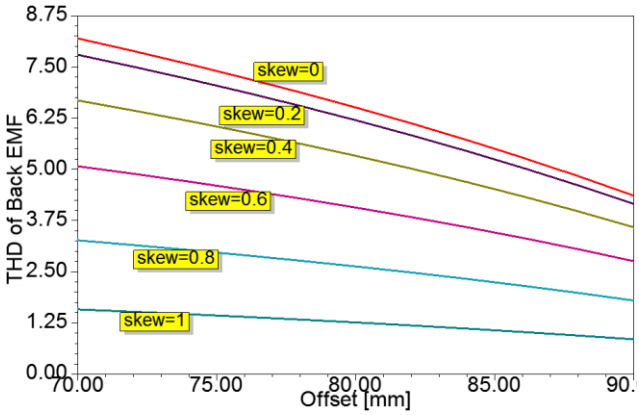


**Fig. 6.** Effect of variable *offset* and *skew* on THD of back emf.

In [32], the effect of varying pole arc to magnet arc ratio $\alpha_m$, magnet thickness and slot opening parameters on the performance of generator have been examined. So, an optimum value of 0.92 for embrace has been found. Since magnet thickness has a powerful effect on terminal voltage, output power, efficiency, cogging torque and power losses; suitable magnet thickness has been obtained via parametric analysis option by considering these parameters. During magnet thickness analyses, it was observed that the machine was running within a wide

range of operation. But, by considering the cost and the distribution of output parameters, the magnet thickness has been chosen as 5 mm. Besides, the slot opening parameter should be wide enough so that the windings are placed into slots easily. On the other hand, narrow slot openings may cause leakage fluxes. In the case that wide slot openings are used, higher cogging torque value may be caused. Through these limits; the slot opening parameter has been set as 2.2mm.

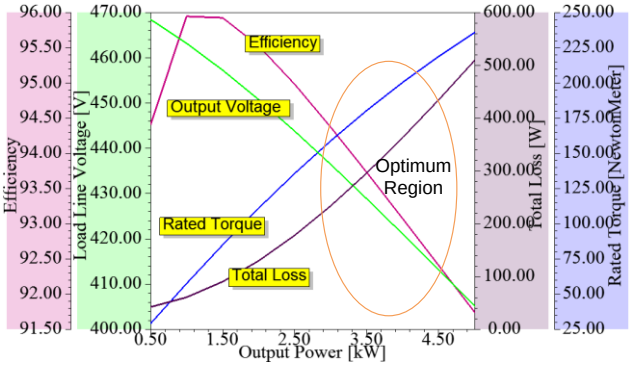


**Fig. 7.** The effect of parameters on generator performance.

By keeping the parameters constant derived as a result of multi-objective optimizations; the output parameters of the machine at rated speed (250 rpm) and different load conditions has been found satisfactory as shown in Fig.7.

## 3. Verification of Analytical And Simulation Model

In this section, the experimental studies and their comparative results are presented in order to verify simulation and analytical results in no-load condition. Coupled electromagnetic field-circuit simulation model used for transient analysis is shown in Fig.8.

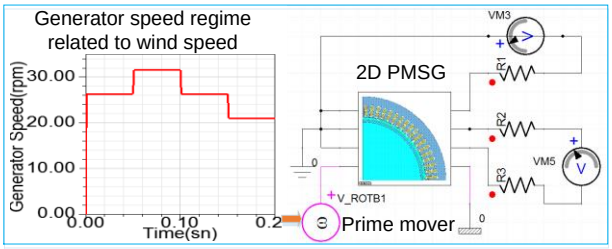


**Fig.8.** Simulation model

The generator speed regime related to wind speed scenario was developed in simulation model as shown in Fig.8. The speed is varied from 200 (rpm) to 300 (rpm) in scenario, and the generator input torque is varied on the basis of the wind speed scenario. The line and phase voltage are presented in Fig.9. It can be noted that the generator is giving an accurate reaction to wind speed changes as shown Fig.9b (simulation) and Fig.11b (experimental).

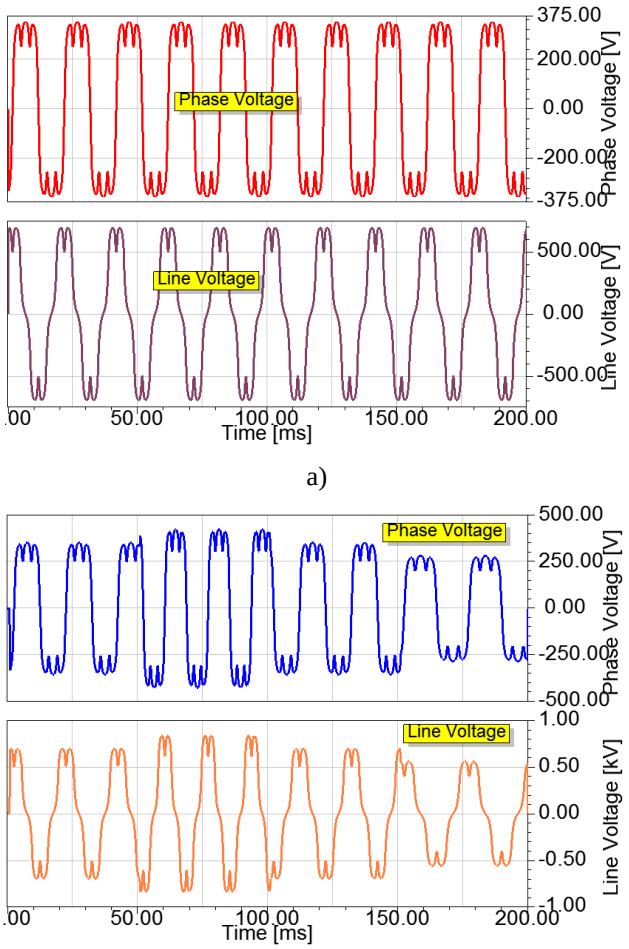


**Fig. 9.** Simulation results derived from no-load operation, a) rated speed (250 rpm) b) variable speed

Fig.10 shows the experimental setup for the verification of the analytical and simulation model proposed. The test setup consists of a 4kW PMSG prototype, an AC motor with reducer as actuator, energy supply, variable speed driver system and measuring elements.

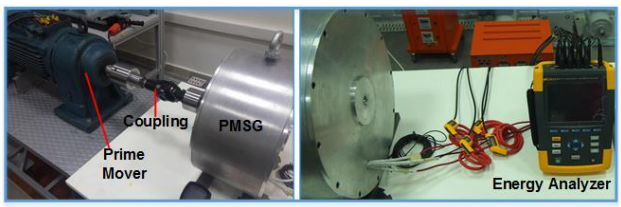


**Fig. 10.** No load test setup of wind generator

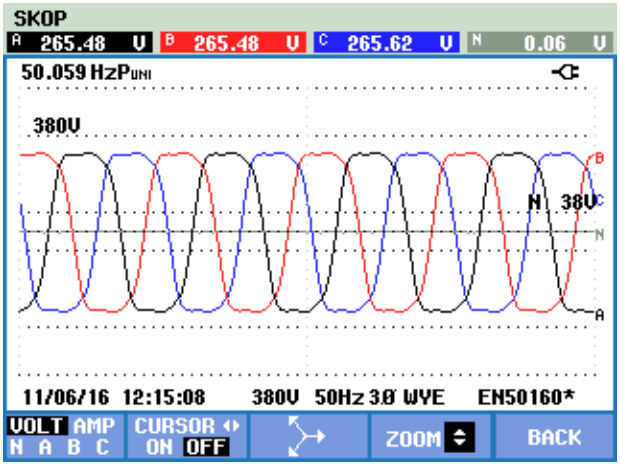


a)

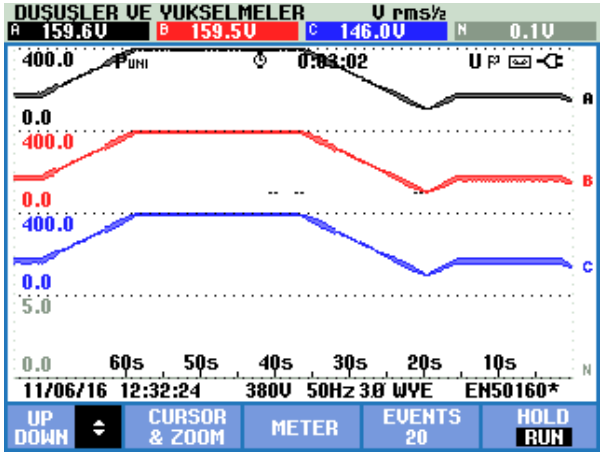


b)

**Fig. 11.** Experimental results under no-load condition: a) induced phase voltages at rated speed (250 rpm), b) induced phase voltages at variable speed

According to the experimental results given in Fig.11, the induced voltage at nominal speed and no-load condition is at desired level. The comparison of the phase and line induced voltage obtained at different speed rates in the simulation, analytical and under no-load test results of the generator is presented in Fig.12.

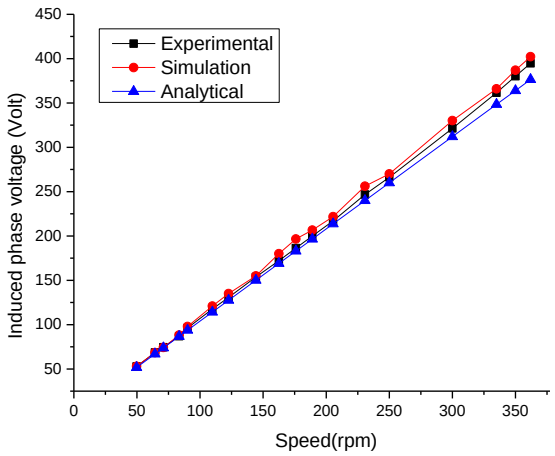


a)

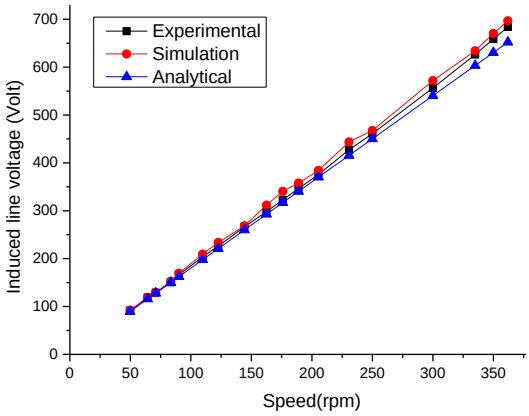


b)

**Fig. 12.** Variation of generator induced voltage relating to varying shaft speed; a) Phase voltage, b) Line voltage

It can be verified through Fig.12 that the experimental results obtained under no-load condition are in good agreement with the analysis and analytical results.

## 4. Conclusion

In this paper, the design of a 4kW permanent magnet synchronous generator suitable for standalone or off-grid wind turbine applications has been developed. The results of analytical PMSG design and concerned optimization methods are reported in the paper. Thereto, the effectiveness of the proposed electrical machine configuration in terms of output power, efficiency, cogging torque and load line voltage have been demonstrated via coupled 2D electromagnetic field-circuit approach by indicating compliance of simulated and no-load conditions prior to the fabrication of the designed and optimized machine. Then, as a part of project; advanced transient analysis studies, the testing and verification of experimental data have been performed following prototyping process. Thus, the proposed analytical approach can reduce the time required for analysis compared with FEM significantly and this may be useful for predicting performance even as initial design process.

## Acknowledgment

This work was supported by the Scientific and Technological Research Council of Turkey (TUBITAK) under grant number EEEAG-113E782. The authors would like to thank TUBITAK for their financial support.

## References

[1] Hossain, J., Hossain, E., Sakib, N., & Bayindir, R. (2017). “Modelling and Simulation of Permanent Magnet Synchronous Generator Wind Turbine: A Step to Microgrid Technology,” International Journal of Renewable Energy Research (IJRER), 7(1), 443-450.

[2] Izelu, C. O., & Oghenevwaire, I. S. (2014, October). “A review on developments in the design and analysis of wind turbine drive trains,” In Renewable Energy Research and Application (ICRERA), 2014 International Conference on (pp. 589-594). IEEE.

[3] Bayhan, S., Fidanboy, H., & Demirbas, S. (2013, October). "Active and reactive power control of grid connected permanent magnet synchronous generator in wind power conversion system," In Renewable Energy Research and Applications (ICRERA), 2013 International Conference on (pp. 1048-1052). IEEE.

[4] Asef, P. (2014, October). "Design, characteristic analysis of PM wind generator based on SMC material for small direct-drive wind energy conversion system," In Renewable Energy Research and Application (ICRERA), 2014 International Conference on (pp. 41-47). IEEE.

[5] Okinda, Victor Omondi, and Nicodemus Abungu Odero. "Modeling, Simulation and Optimal Sizing of a Hybrid Wind, Solar PV Power System in Northern Kenya," International Journal of Renewable Energy Research (IJRER) 6.4 (2016): 1199-1211.

[6] Liang, Q., Yan, X., Liao, X., Cao, S., Zheng, X., Si, H., & Zhang, Y. "Multi-unit hydroelectric generator based on contact electrification and its service behavior," *Nano Energy*, 16, 329–338, (2015).

[7] Camara, M. B., Dakyo, B., Nichita, C., & Barakat, G. "Simulation of a Doubly-Fed Induction Generator with hydro turbine for electrical energy production", *Joint Symposium on Advanced Electromechanical Motion Systems & Electric Drives*, 1-6, (2009).

[8] El-Hasan, Tareq S. "Development of axial flux permanent magnet generator for direct driven micro wind turbine," Renewable Energy Research and Applications (ICRERA), 2016 IEEE International Conference on. IEEE, 2016.

[9] Khan, M. J., Iqbal, M. T., & Quaicoe, J. E. "Tow tank testing and performance evaluation of a permanent magnet generator based small vertical axis hydrokinetic turbine", *Power Symposium*, 1-7, (2008).

[10] Davila-Vilchis, J. M., & Mishra, R. S. "Performance of a hydrokinetic energy system using an axial-flux permanent magnet generator", *Energy*, 65, 631-638, (2014).

[11] Rohmer, J., Sturtzer, G., Knittel, D., Flieller, D., & Renaud, J. "Dynamic model of small hydro plant using archimedes screw", *2015 IEEE International Conference on Industrial Technology (ICIT)*, 987-992, (2015).

[12] Birjandi, A. H., Woods, J., & Bibeau, E. L. "Investigation of macro-turbulent flow structures interaction with a vertical hydrokinetic river turbine", *Renewable Energy*, 48, 183-192, (2012).

[13] Navasardian, A. A. "Underwater hydro unit with the combined energy extraction", *2014 International Conference on Renewable Energy Research and Application (ICRERA)*, 158-161, (2014).

[14] Khan, M. J., Iqbal, M. T., & Quaicoe, J. E. "Dynamics of a vertical axis hydrokinetic energy conversion system with a rectifier coupled multi-pole permanent magnet generator", *IET renewable power generation*, 4(2), 116-127, (2010).

[15] Neely, J. C., Ruehl, K. M., Jepsen, R., Roberts, J. D., Glover, S. F., White, F. E., & Horry, M. L. "Electromechanical emulation of hydrokinetic generators for renewable energy research", *In Oceans*-San Diego, 1-8, (2013).

[16] Khan, M. J., Iqbal, M. T., & Quaicoe, J. E. "Effects of Efficiency Nonlinearity on the Overall Power Extraction: A Case Study of Hydrokinetic-Energy-Conversion Systems", *IEEE Transactions on Energy Conversion*, 26(3), 911-922, (2011).

[17] Broy, A., Tourou, P., & Sourkounis, C. (2015, November). "Transient behaviour and active damping of vibrations in DFIG-based wind turbines during grid disturbances," In Renewable Energy Research and Applications (ICRERA), 2015 International Conference on (pp. 1405-1410). IEEE.

[18] Stegmann, Johannes Abraham, and Maarten J. Kamper. "Design aspects of double-sided rotor radial flux air-cored permanent-magnet wind generator." IEEE Transactions on Industry Applications 47.2 (2011): 767-778.

[19] Tapia, Juan A., et al. "Optimal design of large permanent magnet synchronous generators." IEEE Transactions on Magnetics 49.1 (2013): 642-650.

[20] He, Qingling, and Qunjing Wang. "Optimal design of low-speed permanent magnet generator for wind turbine application." Power and Energy Engineering Conference (APPEEC), 2012 Asia-Pacific. IEEE, 2012.

[21] Tran, Duc-Hoan. "Optimal Sizing of PMSG for Wind Turbine Applications: Methodology and Analysis." Journal of Automation and Control Engineering Vol 3.2 (2015).

[22] Li, Hui, and Zhe Chen. "Design optimization and site matching of direct-drive permanent magnet wind power generator systems." Renewable Energy 34.4 (2009): 1175-1184.

[23] Kilk, A., and A. Kallaste. "Multipole surface-mounted permanent magnet synchronous generators for wind applications." Power Quality and Supply Reliability Conference, 2008. PQ 2008. IEEE, 2008.

[24] Jang, Seok-Myeong, et al. "Design and electromagnetic field characteristic analysis of 1.5 kW small scale wind power generator for substitution of Nd-Fe-B to ferrite permanent magnet." IEEE Transactions on Magnetics 48.11 (2012): 2933-2936.

[25] Wang, Tao, and Qingfeng Wang. "Optimization design of a permanent magnet synchronous generator for a potential energy recovery system." IEEE Transactions on Energy Conversion 27.4 (2012): 856-863.

[26] Lubin, Thierry, Smail Mezani, and Abderrezak Rezzoug. "Improved analytical model for surface-mounted PM motors considering slotting effects and armature reaction." Progress In Electromagnetics Research B 25 (2010): 293-314.

[27] Comanescu, Mihai, Ali Keyhani, and Min Dai. "Design and analysis of 42-V permanent-magnet generator for automotive applications." IEEE Transactions on Energy conversion 18.1 (2003): 107-112.

[28] Heikkilä, Tanja. "Permanent magnet synchronous motor for industrial inverter applications-analysis and design." Acta Universitatis Lappeenrantaensis (2002).

[29] Hsiao, Chun-Yu, Sheng-Nian Yeh, and Jonq-Chin Hwang. "Design of high performance permanent-magnet synchronous wind generators." Energies 7.11 (2014): 7105-7124.

[30] Wanjiku, John Gitonga. Design of an axial-flux generator for a small-scale wind electrolysis plant. Diss. University of Cape Town, 2010.

[31] Daghigh, A., Javadi, H., & Torkaman, H. (2016). "Considering wind speed characteristics in the design of a coreless AFPM synchronous generator," International Journal of Renewable Energy Research (IJRER), 6(1), 263-270.

[32] Cetinceviz, Yucel, Durmus Uygun, and Huseyin Demirel. "Multi-criterion design and 2D cosimulation model of 4 kW PM synchronous generator for standalone run-of-the-river stations." Renewable Energy Research and Applications (ICRERA), 2015 International Conference on. IEEE, 2015.

[33] Upadhayay, P., & Patwardhan, V. (2013, October). "Magnet eddy-current losses in external rotor permanent magnet generator," In Renewable Energy Research and Applications (ICRERA), 2013 International Conference on (pp. 1068-1071). IEEE.

[34] Rahman, M. Azizur, and Ping Zhou. "Analysis of brushless permanent magnet synchronous motors."

IEEE Transactions on Industrial Electronics 43.2 (1996): 256-267.

[35] Strous, T. D. "Design of a permanent magnet radial flux concentrated coil generator for a range extender application." Delft University of Technology, Delft (2010).

[36] Boldea, Ion, and Syed A. Nasar. The induction machine handbook. *CRC press*, 2001.

[37] Faiz, Jawed, and Nariman Zareh. "Optimal Design of a Small Permanent Magnet Wind Generator for Rectified Loads." World Renewable Energy Congress-Sweden; 8-13 May; 2011; LinkÃ¶ ping; Sweden. No. 057. Linköping University Electronic Press, 2011.

[38] Gieras, Jacek F. Permanent magnet motor technology: Design and Applications. *CRC press*, 2002.

[39] Khan, M. A., and P. Pillay. "Design of a PM wind generator, optimised for energy capture over a wide operating range." Electric Machines and Drives, 2005 IEEE International Conference on. IEEE, 2005.

[40] Bianchi, N., and A. Lorenzoni. "Permanent magnet generators for wind power industry: an overall comparison with traditional generators." Opportunities and Advances in International Electric Power Generation, International Conference on (Conf. Publ. No. 419). IET, 1996.

[41] Libert, Florence. "Design, optimization and comparison of permanent magnet motors for a low-speed direct-driven mixer." Licentiate Thesis, Royal Institute of Technology, TRITA-ETS-2004-12, ISSN-1650-674x, Stockholm (2004).

[42] GIERAS, Jacek F.; WANG, Rong-Jie; KAMPER, Maarten J. Axial flux permanent magnet brushless machines. New York, NY: *Springer*, 2008.

[43] Hanselman, Duane C. Brushless permanent magnet motor design. The Writers' Collective, 2003.

[44] Hendershot, James R., and Timothy John Eastham Miller. Design of brushless permanent-magnet motors. Magna Physics Pub., 1994.

[45] Fei, Wei-Zhong. "Permanent magnet synchronous machines with fractional slot and concentrated winding configurations." (2011).

[46] Shao, Mingming, et al. "A lumped parameter magnetic circuit model for fault-tolerant machine with Halbach magnetized permanent-magnet." Electrical Machines and Systems (ICEMS), 2013 International Conference on. IEEE, 2013.

[47] Xu, Peifeng, et al. "Analytical Model of a Dual Rotor Radial Flux Wind Generator Using Ferrite Magnets." Energies 9.9 (2016): 672.

[48] Wang, Daohan, Xiuhe Wang, and Sang-Yong Jung. "Cogging torque minimization and torque ripple suppression in surface-mounted permanent magnet synchronous machines using different magnet widths." IEEE Tran. on Magnetics 49.5 (2013): 2295-2298.

[49] Zhu, Li, et al. "Analytical methods for minimizing cogging torque in permanent-magnet machines." IEEE transactions on magnetics 45.4 (2009): 2023-2031.

[50] Topaloglu, Ismail, et al. "Axial flux permanent magnet generator with low cogging torque for maintenance free under water power generating system." International Journal of Renewable Energy Research (IJRER) 6.2 (2016): 510-519.

[51] Cafieri, Sonia, et al. "Optimal design of electrical machines: mathematical programming formulations." COMPEL-The international journal for computation and mathematics in electrical and electronic engineering 32.3 (2013): 977-996.